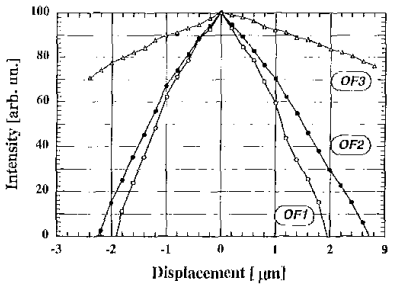

CThM77 Fig. 2. Experimental axial responses obtained when multimode fibers with various core diameters are used. OF1, 50-μm-core-diameter graded-index fiber; OF2, 100-μm-core-diameter graded-index fiber; OF3, 365-μm-core-diameter step-index fiber.

exceeding 0.3 μm. The curves have various slopes because different parts of the out-of-focus signal are introduced into fibers with different core diameter. We attribute the submicron resolution achieved to the extremely large dynamic range of the resolving power. For instance, after a precise fiber adjustment to the maximum signal, we obtain an output power collected by various multimode fibers in the range 0.5–1 mW, which corresponds to 5–10% from the input laser power. Thus, due to the use of apertureless reflection confocal design and large-core fiber for signal detection, a regime of high output power is achieved that provides the high submicron resolution.

1. I.S. Kimura and T. Wilson, "Confocal scanning optical microscope using single-mode fiber for signal detection," Appl. Opt. **30,** 2143–2150 (1991).
2. P. Delaney, M. Harris, R. King, "Fiber-optic laser scanning confocal microscope suitable for fluorescence imaging," Appl. Opt. **33,** 573–577 (1994).
3. M. Ishikawa, Y. Kawata, C. Egami, O. Sugihara, N. Okamoto, M. Tsuchimori, O. Watanabe, "Reflection-type confocal readout for multilayered optical memory," Opt. Lett. **23,** 1781–1783 (1998).

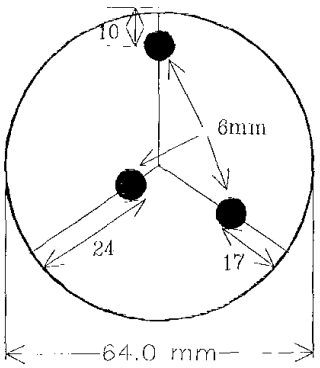

CThM78 Fig. 1. Geometry used for image reconstruction of experimental data.

CThM78 Fig. 2. Absorption image reconstruction using experimental DC data.

time plus computation time spent on reconstruction.

The second aspect is developing a faster Mark II OT system based on multiplexed fibre couplings between source tissue and detector.[1,2]

The Mark I system consists of a single cw light source and a detector, each fiber coupled to a cylindrical, tissue equivalent optical phantom. The light source scans around the phantom and for each source position, the detector scans around the cylinder once. This system is driven by two stepper motors allowing a variable number of measuring positions N.

The phantom used is a perspex cylinder with a diameter of 64 mm. It is filled with a solution of water and Titanium Dioxide particles simulating a scattering medium, plus some ink acting as an absorber. Highly absorbing black metal rods in the solution simulate blood vessels. They are placed as shown in Fig. 1.

The light source is a 35-mW laser diode, emitting at 785 nm. A photo multiplier tube (PMT) is used for detection. DC Data from the PMT is digitized in a computer, which also controls the scanning system and data processing.

Figure 2 shows images obtained from experimental DC data by van der Zee *et al.*[3] These were reconstructed from measurements obtained with $N = 20$ different source/detector positions allowing $N(N-1)$ measurements. N can be varied and changes in image resolution observed. Using the developed source and detection units of the Mark II system, data from AC intensity, amplitude modulation depth and phase is also utilized for this optimization.

The experimental setup is shown in Fig. 3.

This system, also 'rotate rotate', uses multiplexed fiber optics. As an alternative to using multiple sources/detectors,[4,5] light from a single laser diode, amplitude modulated at 200 MHz, is switched to different points around the tissue. This source is multiplexed by an electronically rotatable mirror eliminating the need for a slow stepper motor. Emerging light is collected by fiber-bundles multiplexed into a single detector. Additional heterodyne equipment is used to detect frequency domain data. The first measurements made with this system are used for further image reconstruction.

1. Yuichi Yamashita, Atsushi Maki, Hideaki Koizumi, "A Noninvasive Optical Tomography Measurement System," in *OSA Trends in Optics and Photonics on Advances in Optical Imaging and Photon Migration*, R.R. Alfano and James G. Fujimoto, eds., Vol 2 of OSA Proceedings Series (Optical Society of America, Washington, D.C., 1996), pp. 344–347.
2. R. Salimbeni, G. Marconi, R. Pini, M.

Thursday, May 11

CThM78

Optimization of frequency domain measurement technique and development of a clinical prototype optical tomography system

W. Stanley, P. van der Zee, R. Khalaf,
Department of Physical Sciences, Univ. of Hertfordshire, College Lane, Hatfield, Herts. AL10 9AB, United Kingdom; E-mail: w.r.l.stanley@herts.ac.uk

In order to attempt a clinical evaluation of an optical tomography (OT) system, the scanning time must be kept low. Two aspects of reducing scanning time are looked at in this work.

The first aspect is based on experimentation using an existing system built around a 'rotate rotate' geometry. The aim is to optimize this Mark I system in respect of the number of frequency domain measurements required in order to obtain a reasonably resolved two-dimensional (2D) image. A compromise has to be made between image quality and scanning

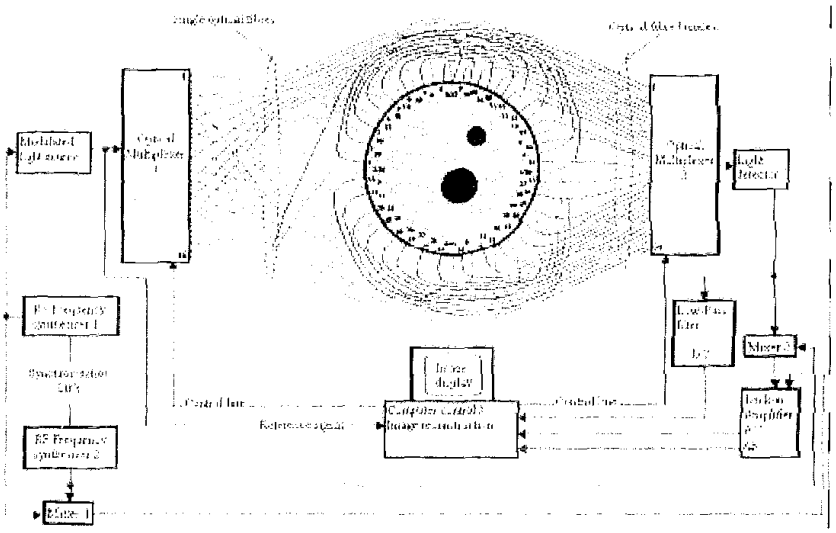

CThM78 Fig. 3. Block diagram of Mark II OT system.

Vannini, "Frequency domain NIR measurements with optical fibers: limits and perspectives," in *Optical Tomography and Spectroscopy of Tissue: Theory, Instrumentation, Model, and Human Studies II*, Britton Chance, Robert R. Alfano, eds., Proc. SPIE **2979**, 676–679 (1997).

3. Pieter van der Zee, Reem Khalaf, Lawrence W.C. Dixon, Alan Davies, "Effect of refractive index and calibration factor on image reconstruction in Optical Tomography," in *Photon Propagation in Tissues IV*, David A. Benaron, M.D., Britton Chance, Marco Ferrari, Matthias Kohl, eds., Proc. SPIE **3566**, 211–221 (1998).
4. Vasilis Ntziachristos, Xu-Hui Ma, Mitchell Schnall, Britton Chance, "A multichannel single photon counting NIR imager for coregistration with MRI," in *Photon Propagation in Tissues III*, David A. Benaron, M.D., Britton Chance, Marco Ferrari, eds., Proc. SPIE **3194**, 219–227 (1998).
5. Quigming Luo, Shoko Nioka, Britton Chance, "Functional Near-InfraRed Imager," in *Optical Tomography and Spectroscopy of Tissue: Theory, Instrumentation, Model, and Human Studies II*, Britton Chance, Robert R. Alfano, eds., Proc. SPIE **2979**, 84–93 (1997).

CThM79

In vivo and *ex vivo* high-resolution evaluation of neoplastic tissues with optical coherence tomography

C. Pitris, W. Drexler, R.K. Ghanta, F.X. Kärtner, U. Morgner, J.G. Fujimoto, A. Goodman,[a] M.E. Brezinski,[a] *Department of Electrical Engineering and Computer Science and Res. Lab. of Electronics, MIT, Cambridge, Massachusetts, 01239, USA; E-mail: cpitris@mit.edu*

Early diagnosis of neoplasia is often critical to improving patient prognosis and successful treating cancer. The imaging capabilities of optical coherence tomography (OCT) make it a promising tool for the early detection of neoplastic changes.[1] Previous studies have evaluated OCT and have demonstrated that microstructural changes associated with neoplasia can be identified.[2,3] These initial findings are very promising and warrant further consideration. The dysplastic human cervix is an excellent model system to systematically investigate and quantitatively evaluate OCT. It is accessible and exhibits well defined pathology, progression and endpoints. Markers of dysplasia and cancer can be identified in the OCT images and their diagnostic utility evaluated. Conclusions can be drawn from studies of the cervix which can be generalized to other epithelial cancers.

In order to evaluate OCT for the detection of micro-structural changes associated with cervical neoplasia *in vivo*, an integrated OCT colposcope was constructed. This instrument permits simultaneous *en face* viewing of structural features while allowing precise registration of the OCT scan plane without interfering with the normal medical procedure. The first clinical feasibility study resulted in successful identification of neoplastic and microstructural changes (Fig. 1). The use of image processing techniques can be a powerful method for analyzing OCT image data, especially when large numbers of patients are involved.[4] Image processing allows complex image information to be reduced to quantitative variables which can be statistically analyzed, quantified, interpreted and used to predict the presence of disease. In addition, it enables faster and better coverage and visualization of large areas and large volumes of data. An example of a segmented OCT image and measurements of some statistical properties are shown in Fig. 2. Those preliminary results appear to correlate with the areas of most advanced neoplasia and could be extended to large volumes of data.

Grading neoplasia will probably require more information than the micro-structural features resolved by standard resolution OCT. Cellular and even sub-cellular characteristics may be critical for the accurate determination of neoplastic grade. A very broad bandwidth $Ti:Al_2O_3$ laser was used for the acquisition of ultrahigh resolution OCT images.[5] The system consisted of a specially balanced and compensated interferometer and achromatic optics. An example of an ex vivo ultrahigh resolution OCT image of the normal cervix is shown in Fig. 3 and demonstrates for the first time, to our knowledge, the presence of cells in human tissue. The squamous cells of the cervical epithelium (arrows), probably with the presence of koilocytosis, are clearly evident in the image. They range in sizes of about 10-30 μm. This finding implies that diagnostically useful cellular information can be extracted from human tissue using a high resolution OCT system.

This paper will describe advancements in the development of OCT as a diagnostic tool for cancer. Key issues to be addressed will be the integration of OCT imaging with currently used diagnostic devices, the use of ultrahigh resolution imaging on the cellular level, and spectroscopically resolved imaging. Examples of *in vitro* and *in vivo* imaging of neoplasia will be presented.

[a]*Massachusetts General Hospital and Harvard Medical School, USA*

1. D. Huang, E. Swanson, C. Lin, J.S. Schuman, W. Stinson, W. Chang, M. Hee, T. Flotte, K. Gregory, C. Puliafito, J. Fujimoto, "Optical coherence tomography," Science **254**, 1178–81 (1991).
2. C. Pitris, A. Goodman, S. Boppart, J. Libus, J. Fujimoto, M. Brezinski, "High-resolution imaging of gynecologic neoplasms using optical coherence tomography," Obstet Gynecol **93**, 135–9 (1999).
3. A.M. Sergeev, V.M. Gelikonov, G.V. Gelikonov, F.I. Feldchtein, R.V. Kuranov, N.D. Gladkova, N.M. Shakhova, L.B. Snopova, A.V. Shakov, I.A. Kuznetzova, A.N. Denisenko, V.V. Pochinko, Yu P.

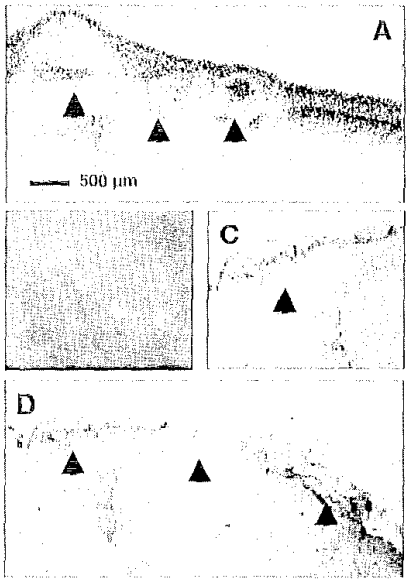

CThM79 Fig. 1. Example of an *in vivo* OCT image of a cervix exhibiting nabothian cysts (A). The arrows indicate the cystis of which correlate well with colposcopy (B) and histology (C 40× & D 20×). This image was acquired using an integrated OCT colposcope at a speed of 4 frames per second. (Wavelength: 1300 nm. Size: 3 × 5 mm. Resolution: 15 μm axial × 22 μm transverse).

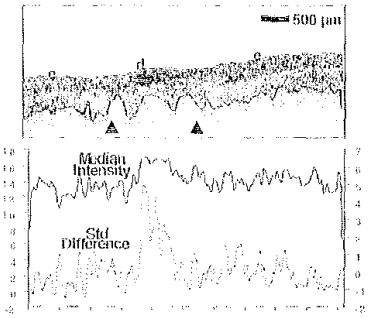

CThM79 Fig. 2. Example of a segmented *in vivo* OCT image of a cervix exhibiting mild focal dysplasia. The arrows indicate the margins of a focal dysplastic area. Normal epithelium (c) and a focal area of dysplasia (d) are visible and correlate well with histology and colposcopy. The OCT image was segmented, using gradient-based filtering and edge detection algorithms, and measurements of the epithelial layer median intensity and standard deviation differences are shown. Analysis of these quantities suggests that areas of focal dysplasia may be identified. (Wavelength: 1300 nm. Resolution: 15 μm axial × 22 μm transverse).

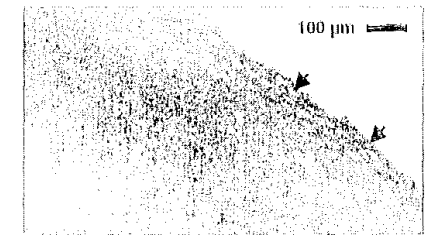

CThM79 Fig. 3. Example of an *ex vivo* ultrahigh resolution OCT image of the normal cervix. The squamous cells of the cervical epithelium (arrows), probably with the presence of koilocytosis, are clearly evident in the image. (Wavelength: 800 nm. Resolution: 1.5 μm axial × 5 μm transverse).